

Atomic Force Microscopy and Specular Reflectance Infrared Spectroscopic Studies of the Surface Structure of Polypropylene Treated with Argon and Oxygen Plasmas

Eun-Deock Seo

Division of Chemical Engineering, Kyungnam University, 449 Wolyong, Masan, Kyungnam 631-701, Korea

Received October 4, 2004; Revised November 15, 2004

Abstract: Isotactic polypropylene (PP) surfaces were modified with argon and oxygen plasmas using a radio-frequency (RF) glow discharge at 240 mTorr and 40 W. The changes in topography and surface structure were investigated by atomic force microscopy (AFM) in conjunction with specular reflectance of infrared (IR) microspectroscopy. Under our operating conditions, the AFM image analysis revealed that longer plasma treatment resulted in significant ablation on the PP surface, regardless of the kind of plasma employed, but the topography was dependent on the nature of the gases. Specular reflectance IR spectroscopic analysis indicated that the constant removal of surface material was an important ablative aspect when using either plasma, but the nature of the ablative behavior and the resultant aging effects were clearly dependent on the choice of plasma. The use of argon plasma resulted in a negligible aging effect; in contrast, the use of oxygen plasma caused a noticeable aging effect, which was due to reactions of trapped or isolated radicals with oxygen in air, and was partly responsible for the increased surface area caused by ablation. The use of oxygen plasma is believed to be an advantageous approach to modifying polymeric materials with functionalized surfaces, e.g., for surface grafting of unsaturated monomers and incorporating oxygen-containing groups onto PP.

Keywords: atomic force microscopy, aging effect, plasma treatment, PP, surface modification.

Introduction

Polymers represent materials of the future. However, their surface properties often do not meet the demands for wettability, biocompatibility, gas transportation and etc. Hence, additional surface modification is required to achieve the desired properties. Plasma-surface modification as an economical and effective materials processing technique has been of scientific and technological interest for over 30 years since it can improve the abovementioned characteristics. The applications for biocompatibility include cleaning, sterilization, deposition or coating, and implantation modification of a substrate.¹ Polypropylene (PP) is not only an important material for conventional uses such as staple fibers, filaments, yarns, technical textiles, and food package but also for specific biomedical uses as suture and integrally molded hinges for finger joint prostheses with an exceptionally high flex life.² In suture application PP causes less infection than other sutures, e.g., stainless steel, chrome catgut, or polyester sutures. The properties of PP fiber depend, to a great extent, on the morphology and surface microstructure of the fibers.

To be used as biomaterials, polymers are generally required to have biocompatibilities with blood and tissues and its compatibilities are also closely related with the surface characteristics such as chemical composition, surface morphology, and wettability, and etc.³⁻¹¹ More importantly, it is believed that the surface morphology plays an important role in biocompatibility of biomaterials *in vivo*. Ohl *et al.*,¹² for example, have reported that the surface morphology of the cell scaffold materials affects the cell behavior and functions. Furthermore, the nature of the substrate material has been found to influence the "D-value" (where D-value is the time necessary to decrease the number of living microorganism by one order of magnitude) of a given microorganism.¹³ At present, plasma techniques are used preferentially to produce different morphology on surfaces to investigate cell biological effects.^{14,15} Thus, it has been of interest to prepare specific polymeric surfaces for applications in the field of biomaterials. The objective of this study is to investigate surface morphological changes in relation with the changes in microstructure of PP surface due to argon-plasma and oxygen plasma treatment by means of atomic force microscopy (AFM) and specular reflectance of infrared microspectroscopy (IMS). AFM and specular reflectance of IMS are particularly powerful tools in the study of surface topography and fine chemical

*e-mail: seo2659@kyungnam.ac.kr

1598-5032/12/608-07©2004 Polymer Society of Korea

structure because AFM can provide high-resolution three-dimensional images of the film surface without any sample pretreatments and damages to the polymer surface, especially enough information on the film surface at the nano level in the height direction,¹² and specular reflectance of IMS also give detailed informations on outermost molecular layer of material without any sample pretreatments and damages to the polymer surface if the sample has a level and lustrous surface.

Experimental

Materials. Isotactic polypropylene (PP) was used as a sheet (Hyosung, Korea). Argon and oxygen gas (purity 99.9%) were purchased from Union Gas. Acetone (spectral grade), which was used as solvent without further purification, was purchased from Sigma Chem. Co.(USA).

Surface Modification Procedures. A capacitatively coupled glow-discharge system, reported elsewhere,¹⁶ with a 13.56 MHz radio-frequency (RF) generator (Auto electronic, Korea, maximum power of 300 W), mass flow controller (MFC, MKS, USA), pressure transducer (MKS Baratron, USA), tubular reactor (76 cm long Pyrex glass tube with 5 cm diameter) and two-stage rotary pump (Welch, USA) were used for the modification of the PP surface.

The PP samples were cleaned first with acetone in Soxhlet extractor and then dried in the tubular reactor under vacuum at room temperature. The reactor chamber was pumped down to 5 mTorr to remove air, moisture and acetone that may have adsorbed on the PP surface and reactor wall. The ablation procedure was carried out by argon gas and oxygen plasma at 240 mTorr, 40 W of discharge power for 1, 3, and 5 min. After plasma treatment, the PPs were cleaned with acetone and then dried under vacuum again. The effects of surface modification by plasma treatments were analyzed by specular reflectance of IMS and AFM.

Instrumental Analysis. In order to obtain the images of argon-, and oxygen-plasma modified surfaces, AFM measurement (Auto Probe CP Research System, USA, equipped with silicone tip) was carried out at room temperature, 40% RH, and at scanning rate of 0.5 Hz in noncontact mode. The mean spring constant of the tip was 17 N/m, the length was 85 μm . Ra (average roughness) was determined as the average deviation of Z values within given areas ($1 \times 1 \mu\text{m}^2$). The PP samples of $1 \times 1 \text{ cm}^2$ size were attached to sample holder with double-sided carbon tape. For the evaluation of changes in chemical structure of the PP surface, Mid infrared (MIR) specular reflectance measurements on samples were carried out on Equinox 55 FT-IR (Bruker GmbH, Germany) equipped with IRscope II in the range of 600-4000 cm^{-1} . The reflectance spectrum obtained was then transformed into absorption spectrum by Kramers-Kronig Transformation (KKT). To ensure that no light is reflected from back surface of the PP, the backside was roughened.

Results and Discussion

Surface Topography by Plasma Exposure. The evolution of the topography observed by AFM for argon-plasma-treated PP and oxygen-plasma-treated PP is shown in Figures 1 and 2, respectively. The oxygen and argon plasma cause an increased removal of the outermost PP regardless of the kind of gas used. However, the topographical alteration demonstrates a significant difference between plasmas employed, and the surface chemical structures, as a result, are also anticipated to be changed. The virgin PP ((A) in Figure 1) has relatively large and bulky ridges, whereas the plasma-treated surfaces develop many new smaller ridges with the treatment time. These observations strongly reveal that some moieties of the polymeric material are ablated more easily than other moieties. Considering the division size of Z scale in Figures 1 and 2, the oxygen-plasma treatment damages PP surface deeply than argon-plasma treatment. In the case of argon-plasma as shown in Figure 1, the sizes of ridges become larger and obtuse but flatten for long treatment duration. The extent of these changes might originate from differences in the surface ablative ability of plasmas between crystalline and amorphous region. Therefore, the ridges in Figures 1 and 2 are assigned to crystallites. This interpretation can be strengthened from the work of Ha *et al.*¹⁷ and agrees well with the results of the literature.¹⁸⁻²⁰

The extent of the roughness, as a measure of alteration, can be monitored quantitatively by instrumental analysis of related data such as Ra and SA values as a function of plasma treatment time, are illustrated in Figure 3. Starting from low Ra value of 2.151 nm for the virgin PP, the Ra values decrease with the treatment time up to 55 and 18% for Ar-plasma and oxygen-plasma treatment, respectively.

The SA values for the oxygen-plasma-treated PP exhibit much higher than that of the virgin PP but slightly decrease and level off at 5 min, whereas those of the counterpart demonstrate lower than that of the virgin PP and decrease with treatment time. The reason for the change in the Ra and SA values between plasmas seems to be closely related with their ablative mechanistic nature on surface physical state such as amorphous and crystallite. Since higher SA values indicate severe and selective ablation at amorphous region, lower SA values is due primary to relatively nonselective ablation regardless of the physical state. As a consequence, the argon-plasma treatment seems to be suitable for obtaining a flat and smooth surface, whereas the oxygen-plasma treatment suitable for obtaining a rough surface as far as surface topography concerns.

It is of value to note the nature of plasmas employed in this study since it could provide clues to elucidate the origin of variations of chemical fine structure on the molecular level basis. By work of Yasuda,²¹ ablation of materials by plasma can occur by two principle processes. One is physical sputtering and the other is chemical etching. The sputtering

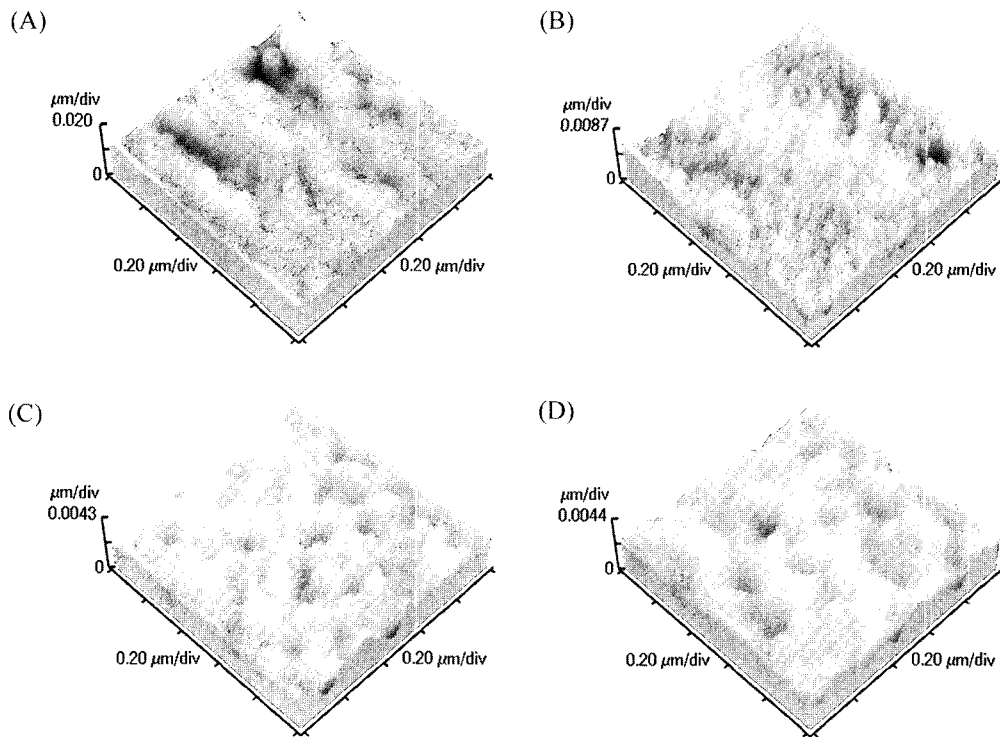


Figure 1. AFM images before and after argon-plasma treatment. (A) virgin PP, (B), (C), and (D) are the surface of argon-plasma treated PP at 240 mTorr, 40 W for 1, 3 and 5 min, respectively.

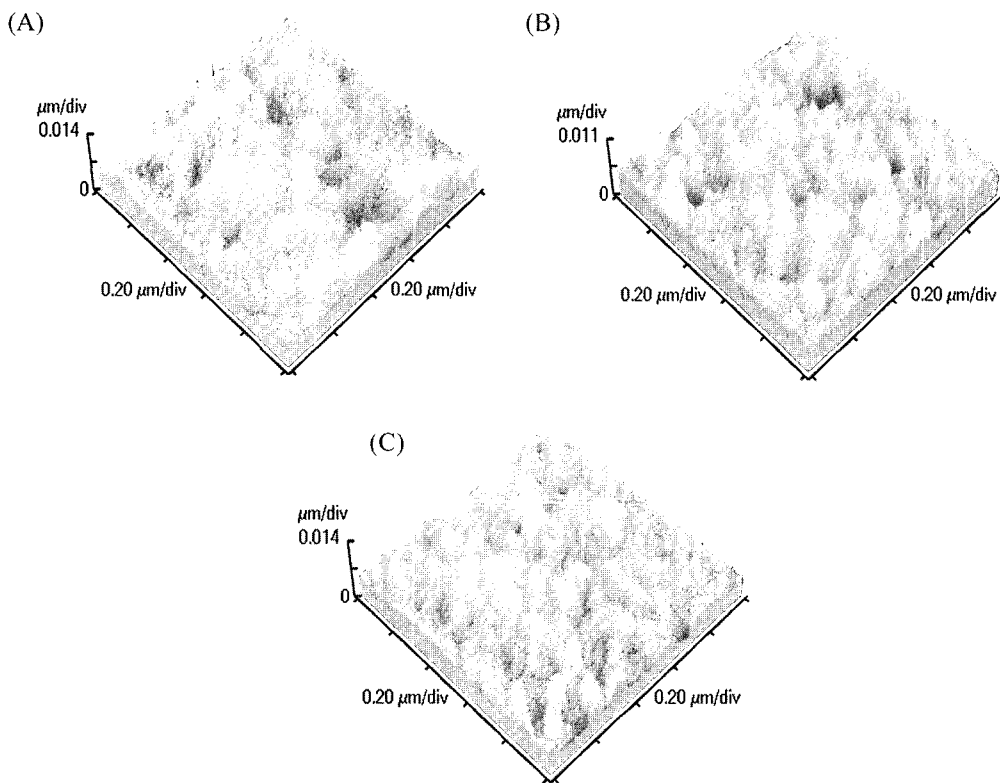


Figure 2. AFM images after oxygen-plasma treatment. (A), (B), and (C) are the surface of oxygen-plasma treated PP at 240 mTorr, 40 W for 1, 3 and 5 min, respectively.

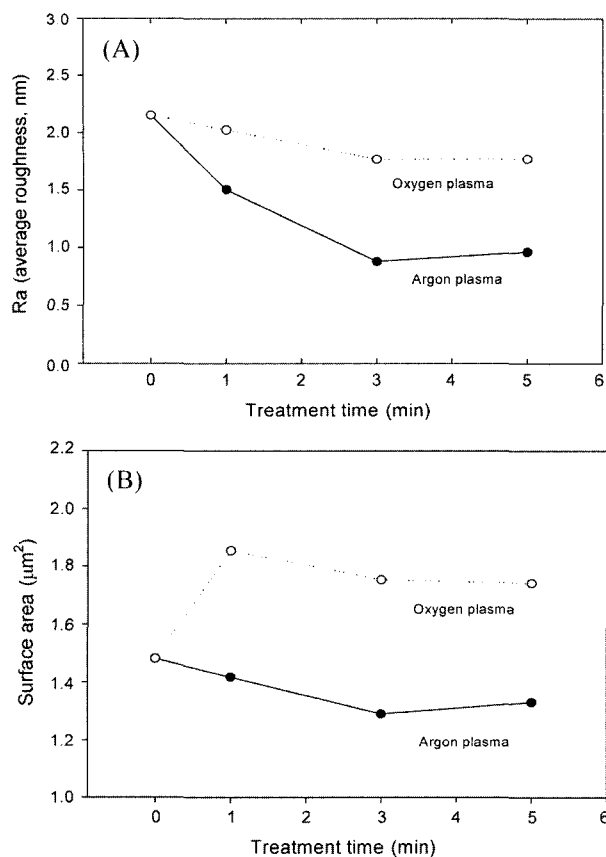


Figure 3. (A) The changes in Ra values, and (B) surface area, with increasing plasma treatment time.

of materials by an inert gas such as argon is a typical example of physical sputtering by a momentum-exchange process, and oxygen is a typical example of chemical etching. After Clouet and Shi,²² in argon-plasma, the argon and excited species can not chemically react with the substrate and the formation of radical is attributed to the ion bombardment, whereas, in oxygen-plasma, atomic oxygen initiates the reaction, beside the ion bombardment, according to PH (polymer) + O → R· + ·OH.

Accordingly, the plasma treatments in this work proceed via different ablative nature: argon-plasma treatment strongly suggests that the ablation takes place through momentum-exchange process, whereas for oxygen-plasma treatment through oxidative degradation by atomic oxygen. In addition to this, coupling of the newly produced surface radicals for both cases might play an important role to alter the topography of the PP surface.

Spectral Analysis. In addition to the topography, to understand the extent and type of chemical modification on the surface due to plasma treatment, reflectance IR spectra are analyzed, which are an appropriate tool for obtaining informations on chemical structure of outermost surface layer materials because plasma modifies the surface of polymer

Table I. Interpretation of IR Absorption Bands for Virgin PP²⁴

Wavenumber (cm ⁻¹)	Interpretation
2957	CH ₃ asymmetrical stretching
2920	CH ₂ asymmetrical stretching
2870	CH ₃ symmetrical stretching, -C-H stretching ²³
2838.40	CH ₂ symmetrical stretching
1455	CH ₃ asymmetrical scissors
1376	CH ₃ symmetrical scissors
1166	3/1 helix structure
974	3/1 helix structure

to a depth of only 1 to 10 μm.²³

Figure 4 shows the IR spectra of (A), the virgin PP, (B), the argon-plasma-treated PP, and (C), the oxygen-plasma-treated PP for 5 min at 240 mTorr, 40 W. Other results with different treatment time are omitted because of no significant differences with those of (B) and (C) in Figure 4. The identification of the absorption bands for the virgin PP is given in Table I. Presence of the same characteristic bands before (A) and after (B, C) plasma treatment indicates that the isotactic nature of PP is not destroyed severely due to the plasma treatments.

The spectrum (D) and (E) in Figure 4, which are difference spectra between the plasma-treated PP and the virgin PP, provide informations on the variations of surface chemical structure by plasma treatments. The spectrum (D) indicates a distinctive variation in absorption bands, for example, hydroxyl band about 3600 cm⁻¹, carbonyl band about 1705 cm⁻¹, and -C-O- band about 1217 cm⁻¹ as well as C-H stretching bands appearing in the range of 2800-3000 cm⁻¹, compared to that of the virgin PP. The hydroxyl, C-O, and carbonyl bands indicate the incorporation of oxygen onto the PP surface. These results agree well with generally accepted mechanism reported in literatures: the first step is free radical formation on the PP surface since the dominant process is hydrogen abstraction in inert gas plasmas and followed by reaction with atmospheric oxygen and/or oxygen containing species (e.g., H₂O) to produce such functionalities.^{22,25}

The spectrum (E) is rather simple compared to the spectrum (D) but shows C-H stretching bands about 3020-2800 cm⁻¹, hydroxyl band about 3600 cm⁻¹, and an additional band about 1650 cm⁻¹, which is presumably due to stretching vibration by carbon-carbon double bond. The existence of the double bond can be supported by presence of =C-H stretching band about 3020 cm⁻¹. From the IR results it can be inferred again that the ablative nature is different depending on plasmas employed as was the case of AFM topography: for hydroxyl band, the spectrum (D) shows more intense absorption than

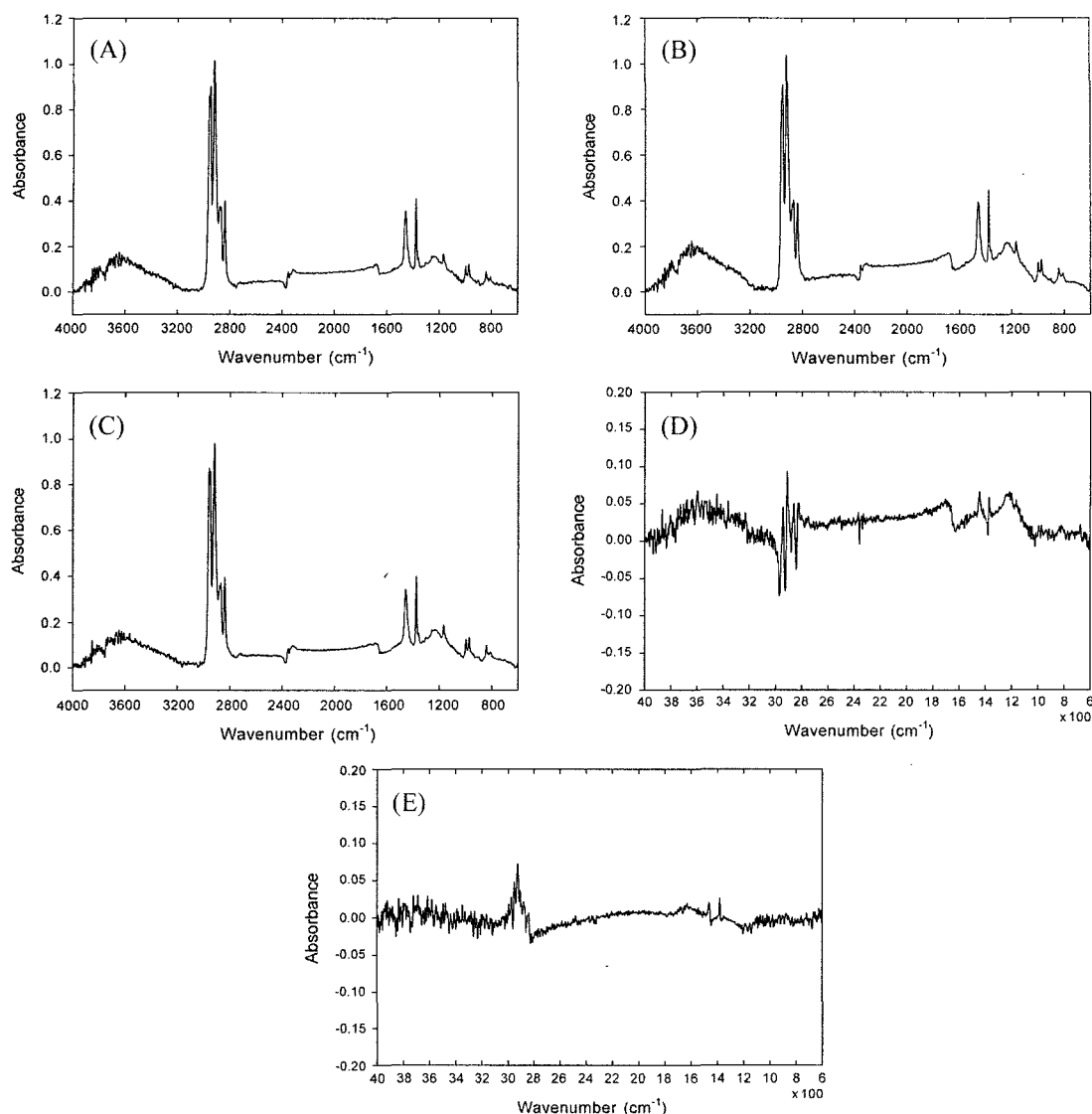


Figure 4. Specular reflectance spectra of PP surface. (A) virgin, (B) argon-plasma-treated for 5 min at 240 mTorr, 40 W, (C) oxygen-plasma-treated for 5 min at 240 mTorr, 40 W, (D) difference spectrum between spectrum (A) and (B), and (E) difference spectrum between spectrum (A) and (C).

the spectrum (E), indicating more sufficient radicals in argon-plasma-treated surface than the counterpart. For C-H stretching band, asymmetric bands decrease whereas symmetric stretching bands increase, indicating argon-plasma affects C-H bonds and thereby significant changes in vibration mode. In the case of oxygen-plasma, C-H stretching bands are, especially $-\text{CH}_2-$ at 2920 cm^{-1} , enhanced, indicating more surface crosslinking occur than the case of argon-plasma.

Aging Effect. It is well-known that in plasma polymerization the gradual increase in oxygen-containing group is caused by the reaction of trapped radical with oxygen.²¹ This phenomenon is one of so-called aging or post-plasma reaction. The IR spectra shown in Figure 5 reveals the aging

effect depending on the treatment time and plasmas employed. Comparing the spectrum (A) and (B) with those of (C) and (D), it is not difficult to find significant differences especially in hydroxyl band and C-H stretching band.

For argon-plasma-treated PP, the aging effect is negligible judging from the hydroxyl bands which show no substantial changes in absorbance for 30 days, hence we can make a conclusion that there are no sufficient surface radicals or trapped radicals to proceed the post-plasma reaction. This observation also leads us to a noteworthy conclusion that in argon plasma treatment the reaction of surface radicals with oxygen in air is completed shortly after exposure of the PP in air. These conclusions agree with those found in the literatures.^{18,26} Poncin-Epaillard *et al.*¹⁸ reported that radicals

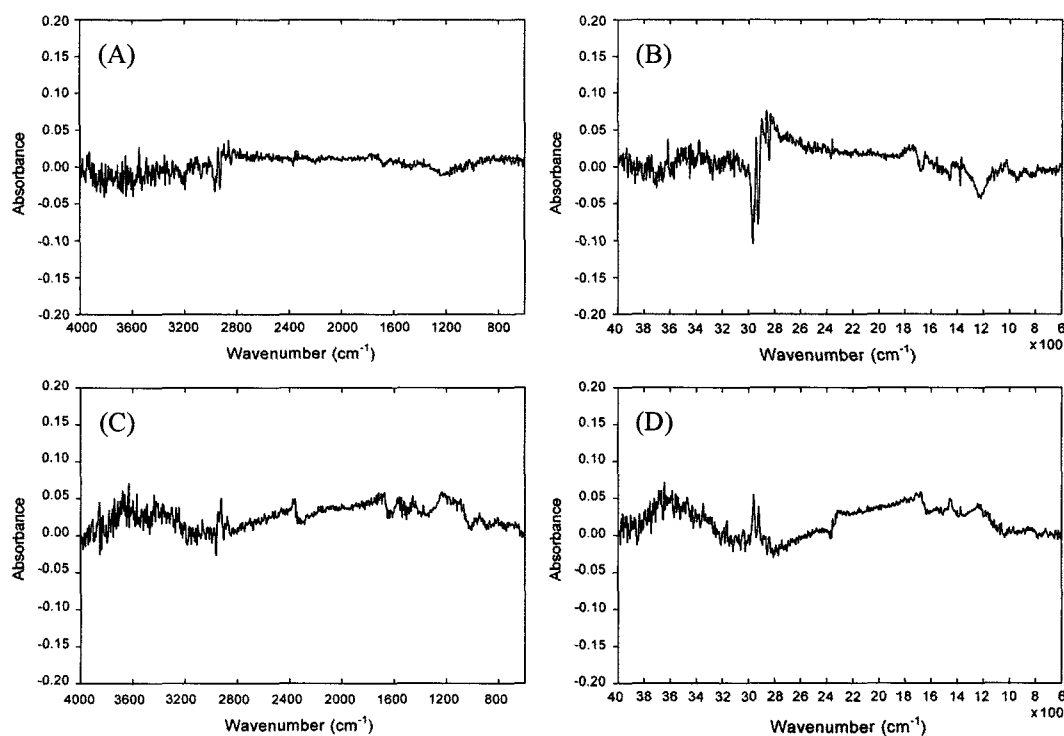


Figure 5. Reflectance spectra showing aging effect, which is obtained from storage for 30 days in air at ambient conditions after plasma treatment, (A) difference spectrum of argon-plasma-treated PP at 240 mTorr, 40 W for 1 min, (B) difference spectrum of argon-plasma-treated PP at 240 mTorr, 40 W for 5 min, (C) difference spectrum of oxygen-plasma-treated PP at 240 mTorr, 40 W for 1 min, and (D) difference spectrum of oxygen-plasma-treated PP at 240 mTorr, 40 W for 5 min.

formed during plasma polymerization decayed within 30 sec. In contrast to the hydroxyl band, C-H stretching modes change appreciably. For example, asymmetric stretching vibrations of $-\text{CH}_3$ and $-\text{CH}_2-$ group about $2960\text{--}2920\text{ cm}^{-1}$ decrease while their symmetrical vibrations about $2840\text{--}2870\text{ cm}^{-1}$ increase. Because this behavior is caused from the variations in vibration mode, it is evident that some changes in surface chemical structure occurred. The most probable explanations on this result are derived from crosslinking by surface radicals formed during argon-plasma treatment, known as CASING (crosslinking by activated species in inert gas plasma)^{27,28} phenomenon, reorientation of mobile group of the PP in the process of reducing surface energy,^{21,23} and partly by newly developed functionalities such as hydroxyl and carbonyl groups, which cause conformational and configurational restrictions on vibration modes, though further studies on which one plays a major role are still await.

On the contrary, the oxygen-plasma-treated PP (spectrum (C) and (D)) clearly exhibits the aging effect, judging from the substantial changes in absorbance of about $3300\text{--}3800\text{ cm}^{-1}$, 1705 cm^{-1} , and about 1217 cm^{-1} corresponding to hydroxyl, carbonyl, and $-\text{C}-\text{O}-$ bands, respectively. Because radicals exposed to environment react promptly with oxygen as mentioned above, these results are due to

reactions of trapped radicals in the PP with oxygen in air, unlikely to argon plasma. This assertion can also be supported by the analysis of AFM result. In case of oxygen-plasma treatment, it ablates PP surface more deeply and severely compared to the counterpart, producing ridges as shown (C) in Figure 2. The ridges shown (C) in Figure 2 are then agglomerated by crosslinking of surface radicals and then isolated surface radicals, which can not take part in crosslinking, might be entrapped into newly developed ridges. The greater SA of ridges by the oxygen-plasma treatment also contribute to the formation of the trapped radicals compared to the case of argon-plasma treatment since the probability for trapping might be anticipated to be proportional to surface area exposed to plasma. Although formulating reliable chemical mechanism for surface modi-

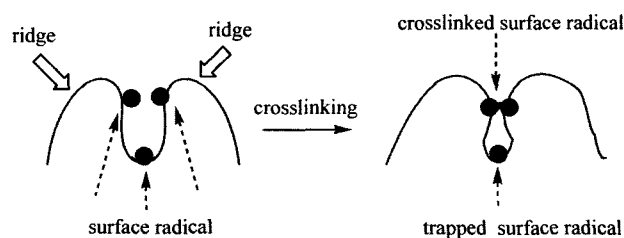


Figure 6. A possible procedure for trapping and crosslinking.

fication is particularly difficult because of the complexity of plasma, one way to account for this behavior is illustrated in Figure 6.

Therefore it can be concluded in this study that argon-plasma treatment leads to enhanced oxygen-containing group and crosslinking and thus more stable surface, whereas the oxygen-plasma produces more surface radicals and in turn, are crosslinked thereby producing many trapped radicals compared to argon-plasma, and that oxygen-plasma might contribute to modifying polymeric surfaces for the preparation of functionalized surfaces, e.g., grafting of unsaturated monomers with various functionalities onto PP.

Conclusions

Isotactic polypropylene was subjected to ablative plasma treatment under argon and oxygen gas, respectively. The changes in AFM topographies of the PP surfaces were investigated in conjunction with reflectance of IMS.

The following results were obtained under our operating conditions. Longer exposure times caused the PP surfaces to damage severely, regardless of the kind of plasma used. In case of oxygen plasma, the surfaces became progressively ablated and showed steep peaks and deep valleys with greater surface area, whereas, for argon-plasma, the surfaces showed a similar ablative behavior but flattened and decreased in surface area with treatment time.

The reflectance IR spectrum analysis showed that a constant removal of surface material was an important ablative aspect for both plasmas but the nature of ablative behaviors and the resultant aging effects were definitely different depending on the plasmas. For argon-plasma, the aging effect was negligible judging from the hydroxyl bands which showed very little changes in absorbance, whereas the oxygen-plasma exhibited aging effect, judging from the increase in the hydroxyl, carbonyl, and -C-O- bands due to post-plasma reactions of trapped or isolated radicals with oxygen in air, reorientation of mobile group, and partly due to the increased surface area. Oxygen-plasma might be a superior mean to modifying polymeric surfaces for the preparation of functionalized surfaces by grafting of unsaturated monomers onto PP.

Acknowledgments. This work was supported by the Kyungnam University Research Fund 2004.

References

- (1) P. K. Chu, J. Y. Chen, L. P. Wang, and N. Huang, *Mater. Sci. Eng. R*, **36**, 143 (2002).
- (2) J. B. Park, *Biomaterials Science and Engineering*, Plenum Press, New York, 1984.
- (3) R. Singhvi, A. Stephanopoulos, and D. J. C. Wang, *Biotechnol. Bioeng.*, **43**, 764 (1994).
- (4) A. F. van Rectum and T. G. van Kooten, *J. Biomater. Sci., Polym. Ed.*, **7**, 181 (1995).
- (5) S. J. Lee, Y. M. Lee, G. Khang, I. Y. Kim, B. Lee, and H. B. Lee, *Macromol. Res.*, **10**, 150 (2002).
- (6) G. Khang, J. M. Lee, P. Shin, I. Y. Kim, B. Lee, Y. M. Lee, H. B. Lee, and I. Lee, *Macromol. Res.*, **10**, 158 (2002).
- (7) G. Khang, J. H. Jeon, J. M. Rhee, and H. B. Lee, *Polymer(Korea)*, **23**, 861 (1999).
- (8) J. S. Lee, G. S. Chae, T. K. An, G. Khang, S. H. Cho, and H. B. Lee, *Macromol. Res.*, **11**, 183 (2003).
- (9) K. E. Ryu, H. Rhim, C. W. Park, H. J. Chun, S. H. Hong, J. J. Kim, and Y. M. Lee, *Macromol. Res.*, **11**, 451 (2003).
- (10) K. S. Yang, X. Guo, W. Meng, J. Y. Hyun, and I. K. Kang, *Macromol. Res.*, **11**, 488 (2003).
- (11) K. E. Ryu, H. Rhim, C. W. Park, H. J. Chun, S. H. Hong, Y. C. Kim, and Y. M. Lee, *Macromol. Res.*, **12**, 46 (2004).
- (12) A. Ohl and K. Schroder, *Surf. Coat. Tech.*, **116**, 820 (1999).
- (13) S. Lerouge, M. R. Wertheimer, and L'H. Yahia, *Plasmas and Polymers*, **6**, 175 (2001).
- (14) H. B. Lee and J. H. Lee, *Biocompatibility of Solid Substrates Based on Surface Wettability*, in *Encyclopedic Handbook of Biomaterials and Bioengineering: Part A. Materials*, D. L. Wise, D. J. Trantolo, D. E. Altobelli, M. J. Yaszemski, J. D. Gresser, and E. R. Schwarz(Eds.), Maecel Dekker, New York, 1995. Vol. 1, pp 371-398.
- (15) G. Khang, M. K. Choi, J. M. Lee, S. J. Lee, H. B. Lee, Y. Iwasaki, N. Nakabayashi, and K. Ishihara, *Korea Polym. J.*, **9**, 107 (2001).
- (16) Y. R. Kang, H. S. Lym, and E. D. Seo, *Polymer(Korea)*, **15**, 570 (1991).
- (17) S. W. Ha, R. Hauert, K. H. Ernst, and E. Wintermantel, *Surf. Coat. Tech.*, **96**, 293 (1997).
- (18) M. Aouinti, P. Bertrand, and F. Poncin-Epaillard, *Plasmas and Polymers*, **8**, 225 (2003).
- (19) S. Vallon, B. Drevillen, and F. Poncin-Epaillard, *Appl. Surf. Sci.*, **108**, 177 (1997).
- (20) E. D. Seo, *Macromol. Res.*, **12**, 134 (2004).
- (21) H. Yasuda, *Plasma Polymerization*, Academic Press, New York, 1985.
- (22) F. Clouet and M. K. Shi, *J. Appl. Polym. Sci.*, **46**, 1955 (1992).
- (23) N. V. Bhat and D. J. Upadhyay, *J. Appl. Polym. Sci.*, **86**, 925 (2002).
- (24) R. Mishra, S. P. Tripathy, K. K. Dwivedi, D. T. Khathing, S. Ghosh, M. Muller, and D. Fink, *Radiation Measurements*, **33**, 845 (2001). see also W. Klopffer, *Introduction to Polymer Spectroscopy*, Springer-Verlag, 1984, p. 91.
- (25) R. M. France and R. D. Short, *Langmuir*, **14**, 4827 (1998).
- (26) D. K. Hegemann, H. Brunner, and C. Oehr, *Plasmas and Polymers*, **6**, 221 (2001).
- (27) H. Schonhorn and H. Hansen, *J. Appl. Polym. Sci.*, **11**, 1461 (1967).
- (28) A. Grill, *Cold Plasma in Materials Fabrication-from Fundamentals to Applications*, IEEE Press, New York, 1994.

Communications

Patterned Fluorescence Images with a *t*-Boc-Protected Coumarin Derivative

Sung-Jun Min, Bum Jun Park, and Jong-Man Kim*

Department of Chemical Engineering, Hanyang University, 17 Haengdang, Seongdong, Seoul 133-791, Korea

Received June 23, 2004; Revised October 6, 2004

Abstract: We have developed an efficient method for the generation of patterned fluorescence images using a protected precursor molecule. The *t*-Boc-protecting group of a coumarin derivative was readily removed from a polymer film upon irradiation with UV light in the presence of a photoacid generator to provide the original properties of the coumarin. Fine fluorescence patterns were obtained when using this photolithographic method.

Keywords: fluorescent image, polymer film, precursor.

Recently, application of photolithographic technology to the generation of patterned functional images has gained much attention in fundamental and applied research areas.¹ The majority of methods reported to date for the patterned functional images rely on so called 'two step procedure'. In the first step, reactive functional groups such as amines or carboxylic acids are produced in the exposed areas by selective irradiation through a photomask. In the second step, the reactive groups generated by photoinduced chemical transformation in the exposed area of the film interact with functional dyes absorbed from the solution. The functional dyes can interact with the reactive moieties by covalent modification, ionic or hydrogen bonding. The 'two step procedure', however, has potential problems such as difficulty of dye penetration into polymer matrices and long-term stability of the patterned images when dye molecules are incorporated into the polymer film by ionic or hydrogen bonding.

In order to avoid these intrinsic problems associated with the 'two step procedure', we² and other groups³ have driven efforts for the development of efficient methods for the functional images without using the wet developing process. We, especially, focused on the so called 'precursor approach' and were able to produce fine fluorescence patterns in the polymer film using the protected precursor molecules. The concept of the 'precursor approach' is to use different electronic properties between the protected and unprotected forms (Figure 1). Thus, a dye molecule is nonfluorescent when the key functional group of the dye molecule is protected with a protecting group (PG). If the protecting group is removed under photoinduced chemical transformation, the fluorescence can be regenerated, allowing patterned flu-

orescent images in the polymer film by selective removal of the protecting group in the exposed areas.

In this communication, as part of our continuing efforts for the development of functional images,² we present a simple but straightforward method for patterned fluorescent images using a *t*-Boc-protected coumarin derivative.

The *t*-Boc-protected precursor molecule **2** used in this investigation was readily prepared by reacting 7-hydroxy-4-methylcoumarin (**1**) with di-*tert*-butyl dicarbonate in pyridine (Figure 2).⁴

Figure 3 shows the absorption spectra of 7-hydroxy-4-methylcoumarin (**1**) and the *t*-Boc-protected precursor **2** in CH₃CN. Although the unprotected coumarin derivative **1** has a longer maximum absorption wavelength (279 nm) than the *t*-Boc-protected precursor molecule **2** (269 nm), the difference is not significant.

The fluorescence spectra, however, show quite different results. As shown in Figure 4, a strong fluorescence emission is observed with the unprotected coumarin **1** while vir-

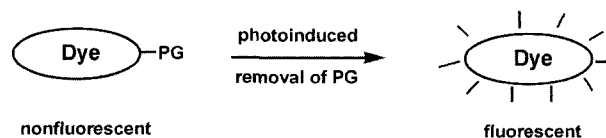


Figure 1. Schematic representation of the concept of the precursor approach for fluorescence images.

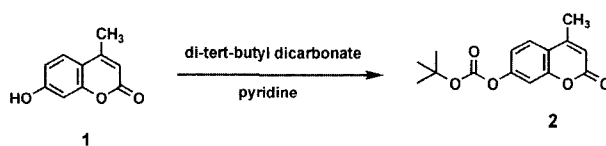


Figure 2. Preparation of the *t*-Boc-protected precursor molecule **2**.

*e-mail: jmk@hanyang.ac.kr

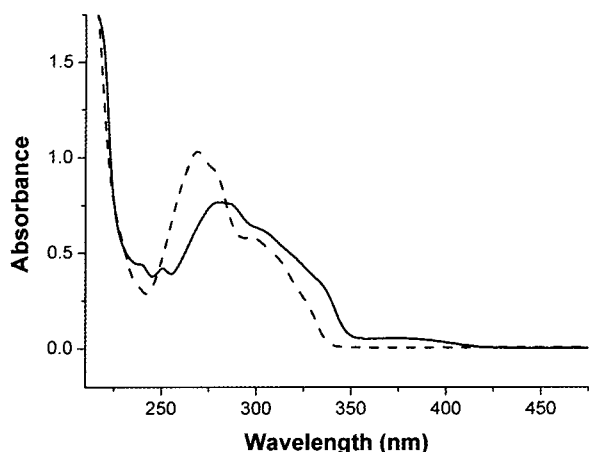


Figure 3. UV spectra of 1×10^{-4} M solution of 7-hydroxy-4-methylcoumarin (**1**) (solid line) and the *t*-Boc-protected coumarin derivative **2** (dotted line) in CH_3CN .

tually no fluorescence is detected with the *t*-Boc-protected precursor molecule **2**. This is quite interesting because if we can convert the precursor molecule **2** to the original molecule **1**, we should be able to regenerate the fluorescence of the unprotected coumarin **1**. The *t*-Boc protecting group in the precursor molecule **2** is acid labile and could be readily removed by photoinduced chemical transformation.

In order to investigate the feasibility of generation of patterned fluorescence images in the polymer film, a photolithographic method utilizing 'chemical amplification method'⁵ was employed. In the chemical amplification process, a catalytic amount of strong acid produced by photodecomposition of a photoacid generator in the exposed area induces a cascade deprotection of the acid-labile protecting groups, typically during the postexposure bake (PEB) step. Accordingly, a dioxane solution containing poly(methyl methacrylate) (PMMA) (79 wt%), the *t*-Boc-protected precursor molecule **2** (20 wt%), and a photoacid generator, triphenylsulfonium hexafluoroantimonate (TPSHFA) (1 wt%) was spin-casted on a silicon wafer. The resulting thin film was exposed to UV light for 1 min through a photomask. Although the thin film contains 20 wt% of the precursor molecule **2**, clean formation of the thin film was observed and maintained after irradiation. No significant color or surface change was observed during the irradiation. After irradiation, the film was subjected to PEB at 100°C for 1 min. As shown in Figure 5, patterned fluorescence images were observed under a fluorescence microscope. The blue areas are the portions exposed through the photomask.

In summary, we have prepared a *t*-Boc-protected coumarin derivative for patterned fluorescence image. The *t*-Boc-protected precursor **2** was readily converted to the unprotected coumarin **1** in the polymer film by photoinduced chemical transformation. Finely-resolved image patterns were obtained when the film was exposed to UV light through a photomask

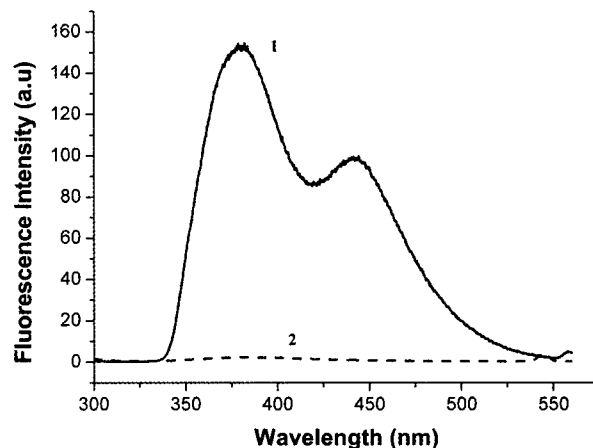


Figure 4. The fluorescence spectra of 1×10^{-4} M solution of 7-hydroxy-4-methylcoumarin (**1**) (solid line) and the *t*-Boc-protected coumarin derivative **2** (dotted line) observed by excitation at 275 nm in CH_3CN .



Figure 5. Fluorescent image patterns obtained with a ca. $1 \mu\text{m}$ thick PMMA film containing the precursor molecule **2** and a photoacid generator on a silicon wafer by contactwise exposure through a photomask as described in the text. The image was obtained after PEB process.

in the presence of a photoacid generator. The simple but straightforward method for the patterned images describe above could be useful for the development of new imaging materials.

Acknowledgments. This research was supported by KOSEF (Center for Ultramicrochemical Process Systems) and MOCIE (Industrial Basic Technology Development Program).

References

- (1) a) A. M. Vekselman, C. Zhang, and G. D. Darling, *Chem.*

- Mater.*, **9**, 1942 (1997). b) M. Schilling, H. E. Katz, F. M. Houlihan, J. M. Kometani, S. M. Stein, and O. Nalamasu, *Macromolecules*, **28**, 110 (1995). c) J.-M. Kim, T. E. Chang, R. H. Park, D. J. Kim, D. K. Han, and K.-D. Ahn, *Chem. Lett.*, 712 (2000).
- (2) a) J.-M. Kim, T. E. Chang, J.-H. Kang, D. K. Han, and K.-D. Ahn, *Adv. Mater.*, **11**, 1499 (1999). b) J.-M. Kim, T. E. Chang, J.-H. Kang, K. H. Park, D. K. Han, and K.-D. Ahn, *Angew. Chem. Int. Ed.*, **39**, 1780 (2000). c) J.-M. Kim, J.-H. Kang, D.-K. Han, C.-W. Lee, and K.-D. Ahn, *Chem. Mater.*, **10**, 2332 (1998). d) J.-H. Lee, I. Cho, K.-D. Ahn, and J.-M. Kim, *Chem. Lett.*, 716 (2001). e) J. Yoo, J.-H. Lee, I. Cho, K.-D. Ahn, and J.-M. Kim, *Macromol. Res.*, **11**, 69 (2003).
- (3) a) S. Kim and S. Y. Park, *Adv. Mater.*, **15**, 1341 (2003), b) C. Coenjarts, O. Garcia, L. Llauger, J. Palfreyman, A. L. Vinette, and J. C. Scaiano, *J. Am. Chem. Soc.*, **125**, 620 (2003). c) N. C. Yang, H. W. Choi, J. K. Lee, J. I. Hwang, and D. H. Suh, *Chem. Lett.*, 824 (2002). d) G. Pistolis, S. Boyatzis, M. Chatzichristidi, and P. Argitis, *Chem. Mater.*, **14**, 790 (2002). e) C.-W. Lee, Z. Yuan, K.-D. Ahn, and S.-H. Lee, *Chem. Mater.*, **14**, 4572 (2002).
- (4) Spectroscopic data for the *t*-Boc-protected precursor **2**: m.p. 93.5 °C ¹H NMR (300MHz, CDCl₃). 1.6 (s, 9H), 2.4 (s, 3H), 6.3 (s, 1H), 7.1 (dd, 1H), 7.3 (s, 1H), 7.6(d, 1H); ¹³C NMR 18.7, 27.5, 84.5, 110.0, 114.3, 114.4, 117.6, 125.3, 150.8, 151.8, 153.3, 154.0, 160.4.
- (5) a) J. M. J. Frechet, E. Eichler, and H. Ito, *Polymer*, **24**, 995 (1983). b) Q. J. Niu and J. M. J. Frechet, *Angew. Chem. Int. Ed.*, **37**, 667 (1998).